A Satellite-derived Climatology of the ITCZ

DUANE E. WALISER

Scripps Institution of Oceanography, University of California at San Diego, La Jolla, California

CATHERINE GAUTIER

Earth Space Research Group, University of California at Santa Barbara, Santa Barbara, California

(Manuscript received 25 June 1992, in final form 29 March 1993)

ABSTRACT

This paper presents fundamental climatological characteristics of the intertropical convergence zone (ITCZ) in a simple concise manner using the highly reflective cloud (HRC) dataset. This satellite-derived dataset uses both visible and infrared observations to measure the frequency of occurrence of large-scale convective systems over the global tropics at a 1° spatial resolution. These dataset characteristics make the HRC particularly well suited for climatological analysis of the ITCZ because the dataset is based on estimates of organized deep convective cloud systems rather than observations of clouds as a whole, and it provides the spatial resolution needed to identify these large-scale convective structures. Furthermore, the dataset covers a time period extending nearly two decades, which provides for a fairly robust climatology and the opportunity to examine seasonal and interannual variability of both the convection and the latitude of the ITCZ.

1. Introduction

Many features of the tropical climate are manifestations of the dynamic and thermodynamic coupling of the Northern and Southern hemispheres. These include equatorial ocean upwelling, large-scale tropospheric deep convection, a complex ocean current structure, the steadiest of atmospheric wind systems, and fast-traveling equatorially trapped waves that result in relatively rapid adjustments to dynamic equilibrium. Of all the various phenomena that characterize the tropical region, the feature that most vividly displays the meeting of the two hemispheres is the intertropical convergence zone (ITCZ). The ITCZ lies in the equatorial trough and constitutes the ascending branch of the Hadley circulation. This permanent low pressure feature marks the meteorological equator where the trade winds, laden with heat and moisture from surface evaporation and sensible heating, converge to form a zone of increased mean convection, cloudiness, and precipitation. The latent heat released in the convective cloud systems of the ITCZ is a critical component of the atmospheric energy balance, and the enhanced cloudiness associated with these cloud systems provides an important contribution to the planetary albedo. Inside and outside the ITCZ, the fluxes of heat, moisture, momentum, and radiation through the surface of the ocean and in the atmosphere itself differ dramatically. Thus, the position, structure, and migration of the ITCZ are important in defining and analyzing the earth's climate on a global scale, and the strength and character of the air–sea coupling on a local scale.

An extensive amount of research on many aspects concerning the ITCZ has been undertaken over the last few decades. The context of these studies varies widely and includes theoretical studies regarding the ITCZ's role in equatorial circulation patterns (e.g., Fletcher 1945; Asnani 1968; Hastenrath 1968), synoptic studies of the ITCZ (e.g., Simpson 1947; Estoque and Douglas 1978; Ramage 1981; Frank 1983), synoptic studies of wave and transient activity within the ITCZ (e.g., Yanai et al. 1968; Reed and Recker 1971; Wallace 1971; Liebmann and Hendon 1990), numerical modeling studies (e.g., Pike 1972; Bates 1970; Goswami et al. 1983), theoretical and modeling studies concerning the latitude of the ITCZ (e.g., Charney 1971; Holton et al. 1971; Hess et al. 1993; Waliser and Somerville 1993), and through modeling studies of the Hadley circulation (e.g., Schneider and Lindzen 1977; Lindzen and Hou 1988; Hack et al. 1989). Although the degree to which the ITCZ has been studied is seemingly exhaustive, there are few consolidated sources of long-record global ITCZ observations and analyses.

After the introduction of satellite imagery to meteorological studies, a number of studies documented the spatial structure and variability of the tropical cloud field (e.g., Kornfield et al. 1967; Hubert et al. 1969; Winston 1971; Gruber 1972). These studies used any-

Corresponding author address: Duane E. Waliser, Institute for Terrestrial and Planetary Atmospheres, Endeavour Hall 129, SUNY, Stony Brook, NY 11794-5000.

© 1993 American Meteorological Society

where from single months to a few years of satellite data and included all cloud types affecting the visible brightness field. Since that time, global-scale analyses focusing on the ITCZ have been rare. The purpose of this paper is to revisit this objective to present and discuss important aspects of global ITCZ climatology in a concise framework. The present study takes advantage of the long-record satellite datasets built up since the last surge of similar works nearly two decades ago, and bases the analysis on a dataset designed to estimate the frequency of occurrence of large-scale convective cloud systems, rather than on a dataset that "measures" the cloud field as a whole. In the next section, the dataset used for this purpose is described. In section 3, the mean spatial structure of the ITCZ is presented and discussed. In section 4, mean meridional profiles of convection and annual cycle variability at several longitudes are compared. In section 5, the mean annual cycle of ITCZ migration at these same longitudes are presented. In section 6, the anomalous fluctuations of ITCZ latitude and intensity over the 17-year record are presented and discussed. Section 7 concludes with a brief summary.

2. Data

The data used in this analysis is the highly reflective cloud (HRC) dataset. This dataset was constructed by Garcia (1985), who used subjectively analyzed daily visible and infrared satellite mosaics (daytime only) to identify the frequency of occurrence of large-scale convective cloud systems (cf. Kilonsky and Ramage 1976). The monthly dataset is composed of "images" where the values denote the number of days in a given month the image elements (geographical areas of $1° \times 1°$) were covered by organized, deep convective systems. Only convective systems extending at least 200 km horizontally were aggregated in the analysis [see Garcia (1985) for details of analysis procedure]. The HRC dataset extends from 25°N to 25°S and from 0° to 359°E. The dataset is currently 204 months long, extending from January 1971 to December 1987 (IR mosaics were not utilized until 1974).

Waliser et al. (1993) have compared the HRC to the outgoing longwave radiation (OLR) dataset (Gruber and Krueger 1984) and the more recently developed International Satellite Cloud Climatology Project (ISCCP) Stage C2 convective cloud dataset (Rossow and Schiffer 1991). That study compared and discussed dataset creation procedures, spatial and temporal scales of analysis, frequency-dependent variability, biases, and the local relationships to sea surface temperature. As a measure of monthly deep convection, Waliser et al. found the HRC to be in good qualitative agreement with the ISCCP C2 convective cloud data on monthly time scales, especially in regions of intense deep convection such as the ITCZ. Further, the study found the HRC to be equally adept as, and often superior to, the OLR for large-scale studies of convection, especially in regions of widely different tropical climate regimes. The results from that study, along with the HRC's 17-year record length and one degree spatial resolution, indicate that the HRC is very well suited to describe the ITCZ mean structure, and its temporal and spatial variability on the scales characteristic of the large-scale organized convective systems (i.e., 1–5 days, 100–1000 km) of which it is composed.

The sea surface temperature (SST) data combine an in situ measurement analysis from 1975–1981 with a blended analysis of satellite-derived and in situ measurements from 1982–87 (Reynolds 1988).

3. Mean spatial structure

Figure 1 shows the January, April, July, and October mean monthly HRC fields, each computed from the average of 17 monthly images (1971–87). These four maps illustrate the structure and mean migration pattern of the ITCZ throughout the year. The HRC values range between 0 and 13 days per month, with the greatest values occurring in and near summer monsoon–driven circulations and the lowest occurring under persistent high pressure zones, such as the South

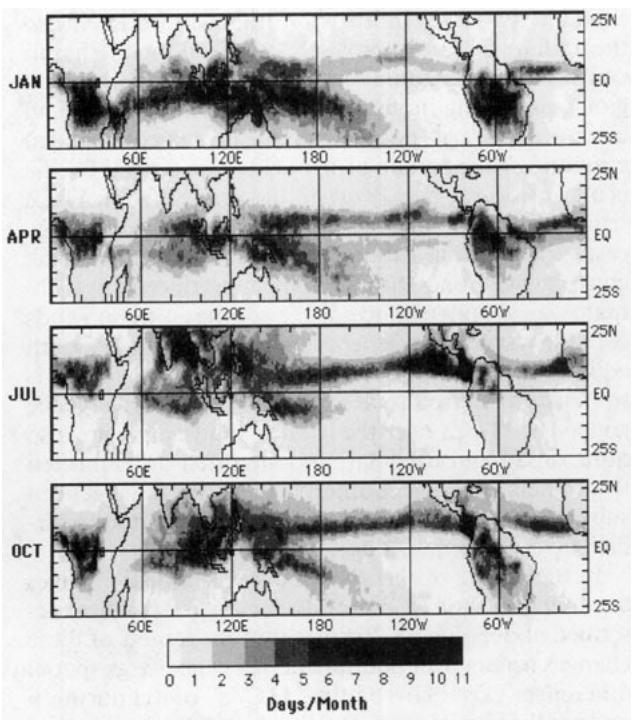

FIG. 1. Mean monthly "ITCZ" structure for the months: (a) January, (b) April, (c) July, and (d) October. These mean monthly images were computed from 17 years of monthly HRC data. Values represent the number of days per month (sampled once per day) the given grid point was covered by a large-scale deep convective system (subjectively determined; see section 2).

Pacific high. On a global scale the ITCZ could be described as a near-solid convective cloud band encircling the earth near the equator. The maps show that this "cloud band" tends to favor the Northern Hemisphere at most longitudes. The reason for this hemispheric preference has rarely been addressed directly. The preference for warm SSTs ($> \sim 27°C$) in the tropics to also favor the Northern Hemisphere (Levitus 1982), along with the tendency of large-scale convection to occur in regions of high SST (e.g., Graham and Barnett 1987), suggests that local forcing conditions likely play an important role. Flohn (1971) suggested that the north–south asymmetry in the ITCZ resulted from the Southern Hemisphere's greater baroclinity. This asymmetry in baroclinity could result from the greater amount of landmass in the Northern Hemisphere and/or the more extensive ice sheets in the Southern Hemisphere. Using a simplified model of the hemispheric heat balance, Kraus (1977) concluded that "the position of the ITCZ is probably affected by the global heat balance distribution and not simply by local conditions."

Beyond the ITCZ's gross zonal symmetry, there are a number of distinctly different ITCZ regimes. Over the Atlantic and eastern Pacific oceans, nearly half the globe, the ITCZ is characterized by a narrow well-defined cloud band—a structure that conforms to the traditional or conceptual notion of an ITCZ. In contrast, the ITCZ extending from the western Pacific to the Indian Ocean is broader in latitude with significantly more horizontal spatial variation. In these regions, the strong monsoon flows, Indonesian low, and large ocean warm pools wash out the narrow banded structure of the archetypical ITCZ. The central Pacific is a transition region between the very different ITCZ structures to the east and west. It contains a southeastward-pointing extension called the South Pacific convergence zone (SPCZ) that is produced by a climatological convergence of the southeast trade winds over the warm water generally associated with the south equatorial countercurrent. This convergence zone is sometimes referred to as an intratropical convergence zone. The ITCZs over the tropical landmasses are also quite broad and irregular, and are often disconnected from their oceanic counterparts by the convection-suppressing influence of cold water brought to the surface by coastal upwelling.

In the course of the annual cycle, seasonal changes occurring in the ITCZ modify the mean structure described above. Figure 1 shows that the largest of these changes occurs over South America where large spatial differences exist between the "ITCZs" of the northern and southern summers. During the southern summer, the rainy season envelops nearly the entire tropical area of the South American continent. This produces a latitudinally and longitudinally broad ITCZ. In the northern summer, the ITCZ overlies the oceanic region north of the continent and has a structure more consistent with its ocean counterparts to the east and west. Another dramatic seasonal change in the ITCZ structure occurs in and near the Indian Ocean during the Asian summer monsoon. The monsoon circulation decouples the ITCZ proper from the intense monsoon-driven convection centered over Southeast Asia. A similar enhancement of convection occurs in the southern summer over northern Australia, however the structural change to the ITCZ is not as dramatic. During this same season, the convergence zones over Africa and the Indian Ocean become well connected due to the reduced coastal upwelling off the East African coast. Other modest seasonal deviations occur in the eastern Pacific during the northern spring, when the ITCZ occasionally develops as two zones of convection straddling the equator. This double ITCZ results from a relaxation of the southeast trades that greatly diminishes the equatorial and nearby coastal upwelling, leaving seasonably warm surface temperatures south of the equator. In a related manner, the two branches of convergence in the central Pacific oscillate in strength during the year with the southern and northern branches intensifying during their respective summer seasons.

The overall annual north–south migration pattern of the ITCZ is also depicted by the four maps in Fig. 1. In general, the entire line-oriented convection band marches north in the northern spring and summer, and south in the southern spring and summer. The differences in the amplitudes and phases of the ITCZ excursions at different longitudes emphasize the different atmospheric and surface forcing regimes. The ITCZ over land (Africa and South America) follows the annual march of the sun. This pattern is also exhibited, although to a lesser degree, in the ITCZ migration over the Indian and western Pacific oceans. In these regions strong monsoon circulations driven by large land–ocean temperature differences play a substantial role in the spatial and temporal distribution of convection (e.g. Webster 1987). The ITCZ migration over extended ocean regions lags slightly behind the ITCZs over land. This time lag is most apparent in the eastern Pacific and the Atlantic oceans, where the ITCZ is farthest south in the northern spring and farthest north in the northern fall. The origin of this time lag is presumably due to the large thermal inertia of the ocean compared to land and to the dynamic inertia of the wind-forced surface current structure of the equatorial oceans. These currents, particularly the warm North Equatorial Countercurrents, play a significant role in determining the spatial structure and location of the time-mean convection field. A more detailed consideration of the ITCZ migration patterns will be presented in sections 5 and 6.

The maps of mean convection shown in Fig. 1 depict the global nature of the ITCZ and offer a glimpse at the temporal and spatial variability of this ubiquitous tropical feature. In the following two sections, the spa-

tial and temporal characteristics of the ITCZ at different longitudes will be analyzed in more detail. For this purpose, seven nonoverlapping ITCZ regions, in addition to the globally averaged ITCZ, have been selected for analysis. The seven regions are intended to represent different tropical land–ocean–atmosphere climate domains. The zonal extents of these regions were chosen to provide consistency in terms of the atmospheric circulation pattern, surface type, and ocean current structure within each region. The longitude limits of the selected regions and their denotations are given in Table 1.

TABLE 1. Labels and longitude limits for ITCZ domains analyzed. Latitude limits are 25°N and 25°S.

Label	Longitude limits
Africa	10°–40°E
Indian	60°–100°E
West Pacific	110°–150°E
Central Pacific	160°E–160°W
East Pacific	100°–140°W
South America	45°–75°W
Atlantic	10°–40°W
Global	0°–359°E

4. Meridional profiles

Figure 2 shows the mean meridional profiles of deep convection within the ITCZ for the eight domains specified in Table 1. These profiles (thick lines) were computed by averaging the HRC within the given longitude limits over all 204 months of data. The standard deviation of the annual cycle (thin lines) about its respective mean profile is also given, where the annual cycle is the sequence of 12 mean monthly (January–December) meridional profiles. The first seven plots (2a–g) are presented in order of increasing eastward longitude (i.e., Africa to the Atlantic Ocean). The eighth plot (2h) illustrates the mean and standard deviation profiles for the globally averaged ITCZ.

The mean meridional profiles of convection each show peak amplitudes of about three to four days per month. These peak values generally occur between the latitudes of about 8°N and 8°S; however, they rarely occur over the equator and are often found to straddle the equator over oceanic regions. This characteristic has most often been attributed to the distribution of sea surface temperature (SST), specifically the convection-suppressing influence of cool sea surface temperatures associated with equatorial upwelling (e.g., Bjerknes et al. 1969). For example, this feature is most pronounced over the central and eastern Pacific and Atlantic oceans (2d, e, g), where relatively steady and strong easterly trades force considerable equatorial upwelling. However, a similar feature is apparent in the warm-pool regions of the western Pacific and Indian oceans (2b,c) where there is no surface signature of equatorial upwelling.[1] Figure 3 shows the mean meridional profiles of SST and HRC from four of the oceanic domains. From these plots, it is clear that equatorial upwelling is not a characteristic feature in the warm-pool regions. This is presumably due to the relatively deeper isothermal layer (Levitus 1982) and weaker easterly winds in this part of the tropics (Legler and O'Brien 1984). The suppression of large-scale atmospheric convection at the equator over the tropical warm pools highlighted in Figs. 2b and 2c is not a well-documented feature, particularly over long time scales. In these regions, the data suggest that a dynamic mechanism of atmospheric origin has a suppressing influence on convection at the equator, or alternatively, an enhancing influence just off the equator. Theories that may explain this off-equatorial enhancement of convection, and/or an ITCZ away from the equator, have been given by Charney (1971), Holton et al. (1971), Lindzen (1974), and Waliser and Somerville (1993).

In general, the meridional profiles shown in Fig. 2 are characterized by one of the following forms: a rather broad profile nearly symmetric about the equator, a narrow profile with its peak located in the Northern Hemisphere, or in the case of the central Pacific (2d), a strong, nearly symmetric double peak in convection. The structure of these profiles to a large degree reflects the structure of the underlying mean meridional surface temperature profile, as was shown in Fig. 3. The mean profile over Africa (2a) has peak convection nearly centered over the equator, and is the most symmetric of the profiles presented. The slight asymmetry in this region results from the exceedingly dry climate of the Sahara desert north of about 15°N. The profile over the Indian Ocean (2b) is markedly asymmetric about the equator. The maps of Fig. 1 show that during the southern summer, convection is strongly enhanced just south of the equator, while in the northern summer, the monsoon over India displaces a considerable amount of convection to the Indian subcontinent; convection that would otherwise occur in the near-equatorial region. Monsoon circulations also influence the mean profile of the western Pacific (2c); however, the influence is more symmetric due to summer monsoons occurring over both southern Asia in July and northern Australia near January. Thus, the mean profile over the western Pacific is nearly symmetric and only slightly displaced to the Northern Hemisphere.

The profiles of the central and eastern Pacific Ocean and the Atlantic Ocean (2d,e,g) are cases where the SST distribution appears to play a particularly important role in the meridional profiles of convection (Fig. 3). South America (2f) is a unique case, since the underlying surface changes considerably with latitude,

[1] This particular feature has been found to exist in overlapping outgoing longwave radiation data (another proxy of deep convection) and ISCCP C2 deep convection data, and therefore is not believed to be an artifact of the convection index used here.

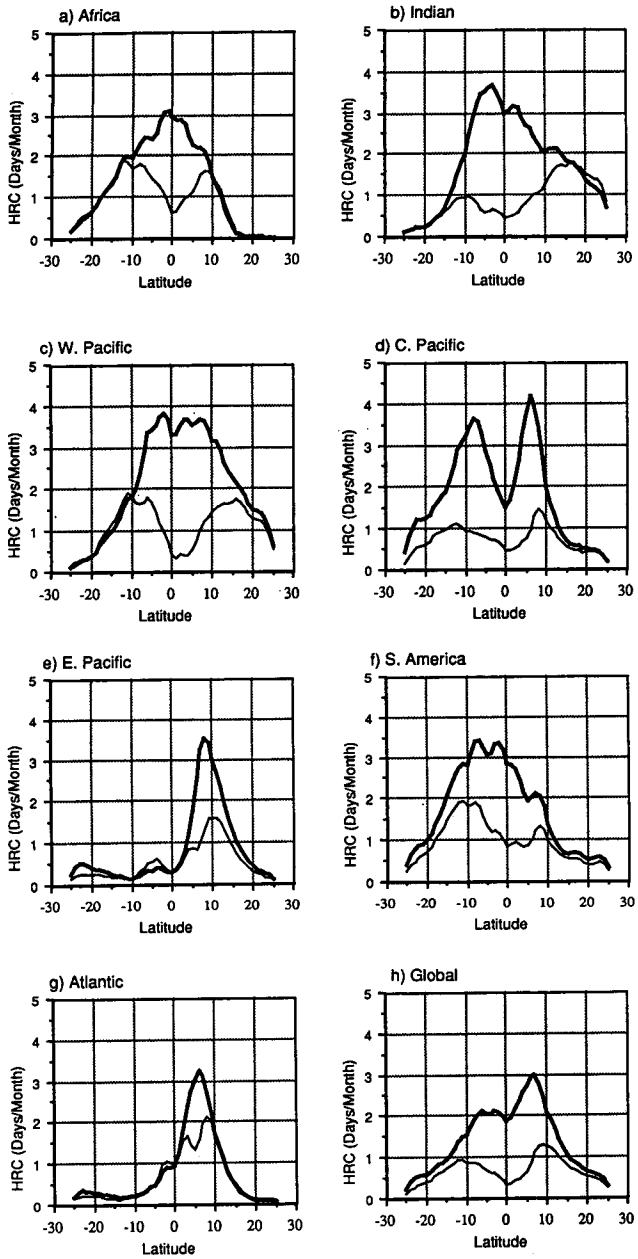

FIG. 2. Mean meridional profiles of HRC for the regions given in Table 1 (thick lines). These profiles are the zonal and temporal average HRC computed over the longitude limits specified in Table 1 and over all 204 months of data. The standard deviation of the annual cycle (SDAC; thin line) is also shown. The SDAC was computed from the standard deviation of the 12 (January–December) mean monthly profiles about the overall mean profile.

consisting of mostly ocean north of the equator and mostly land south of the equator. Within this region, the organization of large-scale convection is weakened during the northern summer due to the monsoon occurring over central America. The circulation pattern associated with this monsoon enhances convection over Central America and suppresses convection in the region north of South America. The global profile (2h) consists of a meridionally broad profile with a strong convection maximum occurring in the Northern Hemisphere at about 6°N.

The dominant seasonal modifications in the ITCZ mean structure were illustrated in Fig. 1 and discussed briefly in section 3. The profiles of standard deviation within the annual cycle (hereafter SDAC) shown in the plots of Fig. 2 (thin lines) depict these changes in a more quantitative way. Large seasonal modifications to the ITCZ structure are indicated by asymmetries in the SDAC profiles about the equator. The SDAC profile for the Indian Ocean (2b) shows such an asymmetry; large variability exists north of about 10°N, almost twice as much as in the Southern Hemisphere at this latitude. This illustrates the strong seasonal enhancement of convection over the Indian subcontinent due to the summer monsoon. South America (2f) is another region with large asymmetries in the SDAC. In this region, the annual cycle has a strong seasonal response at about 10°S due to the rainy season enveloping the Amazon basin during the austral summer. The SDAC profiles for Africa and the west and central Pacific (2a,c,d) are all quite symmetric about the equator. In these regions, the structure of the ITCZ remains essentially the same throughout the annual cycle with the seasonal variations being mostly in the form of north–south oscillations. The east Pacific and Atlantic SDAC profiles (2e,g), on the other hand, are cases where very little north–south migration occurs and seasonal variability consists mostly of changes in convection intensity—weak in the boreal spring and strong in the boreal fall. In addition, the eastern Pacific shows a mild peak

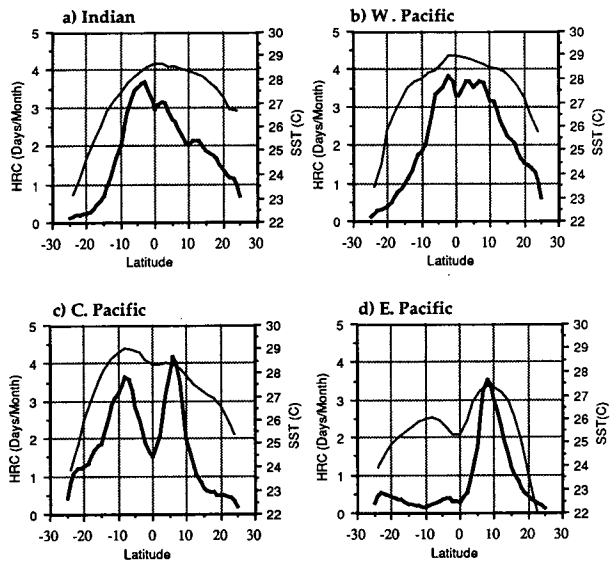

FIG. 3. Long-term (1971–1987) mean meridional profiles of HRC and SST for the regions denoted in Table 1 as: (a) Indian, (b) west Pacific, (c) central Pacific, and (d) east Pacific. HRC and SST data have 1° and 2° resolution, respectively.

in variability at about 5°S due to the occasional formation of a double ITCZ in the boreal spring. The SDAC profile of the global ITCZ (2h) shows variability indicative of the annual north–south migration of the tropical convergence zones with slightly more variability in the Northern Hemisphere due to the contributions from the eastern Pacific, Atlantic, and Indian Ocean regions. A more detailed analysis of the frequency-dependent variability of the HRC is given in Waliser et al. (1993).

5. Mean meridional migration of the ITCZ(s)

As discussed in the Introduction, the position and intensity of the ITCZ strongly influence the character and strength of the large-scale circulation and the local air–sea coupling. The purpose of this section is to analyze and document the mean meridional migration patterns of the ITCZ at several longitudes. Figure 4 shows time–latitude diagrams of the mean annual cycle of the ITCZ for the eight domains given in Table 1. The plots are presented in the same order, beginning with Africa (4a), increasing in longitude to the Atlantic (4g), and ending with the global ITCZ (4h). These diagrams were constructed from the sequence of 12 (January–December) mean monthly zonally averaged HRC profiles, and thus provide an estimate of the latitude and relative intensity of the ITCZ throughout the annual cycle. The HRC values range from zero days per month (white) to about seven days per month (black). The white line overlaying each diagram gives a quantitative estimate of the mean meridional migration of the ITCZ, and was constructed as follows. For each month, the ITCZ latitude ($\bar{\theta}$) is calculated as the HRC-weighted mean latitude;

$$\overline{\theta(t)} = \frac{\int_{-25}^{+25} H(\theta,t)\cdot\theta d\theta}{\int_{-25}^{+25} H(\theta,t) d\theta},$$

where t is the month index spanning the 204 months of HRC data; H is the zonally averaged HRC over the given longitude domain; and θ represents latitude in degrees [cf. Gadgil and Guruprasad (1990) for other methods of determining ITCZ latitude]. The mean annual cycle of ITCZ latitude is then computed from the 204-month time series (17 years) of ITCZ latitude. Note that the time series of ITCZ latitude was not computed for the central Pacific region (4d) since the structure in this region is inherently double banded and thus the notion of a single ITCZ latitude does not apply.

Figure 4a shows that the annual cycle of the ITCZ over Africa exhibits a migration pattern that has a nearly sinusoidal nature. In this region the ITCZ appears to be in near-perfect phase with the solar cycle of surface heating, migrates from about 10°N to 10°S, and has a very even intensity throughout the cycle (about 4 days month^{-1}). The Sahara desert in northern Africa appears to inhibit the northern migration of the ITCZ, and slightly suppress its intensity while in the Northern Hemisphere. In contrast to this nearly sinusoidal case, all other regions (4b–g) show an ITCZ annual cycle that has seasonal dependencies in intensity, structure, and/or an overall phase lag relative to the surface solar heating cycle. For example, the ITCZ migrations over the Indian (4b) and western Pacific (4c) oceans show convection intensification associated with the summer monsoons occurring in those regions. The Asian summer monsoon produces a significant enhancement to the convection in the northern summer months, which in the case of the Indian Ocean produces two bands of large-scale convection, one near the equator and one near southern India. The annual cycle of the ITCZ in these two regions lags approximately one month behind the solar heating cycle, presumably due to the thermal inertia within these predominantly ocean regions.

The eastern Pacific (4e) and Atlantic (4g) oceans have very similar annual cycles. As suggested earlier by Figs. 1 and 2, the ITCZ in these regions remains primarily in the Northern Hemisphere throughout the year, with some light convection (~2 days month^{-1}) occurring south of the equator in the boreal spring. During this time of year, warm water (~27°C or greater) occurs on both sides of the equator in this region and the ITCZ, in its southernmost position, is split by a zone equatorial upwelling (i.e., cool equatorial surface temperatures). The phase of the annual cycle in these regions lags behind the surface solar heating cycle by approximately two months, and each produces the most intense ITCZ in the boreal fall. During this season, the surface water associated with the equatorial countercurrents is warmest, and the Hadley circulation and low-level trade wind convergence are strongest (Oort 1983; Legler and O'Brien 1984).

The annual cycle of the central Pacific and South America shows very different characteristics from those described above. As illustrated earlier in Figs. 1 and 2, the ITCZ in the central Pacific is composed of northern and southern convergence zones straddling the equator. While this large-scale "double" convergence zone remains intact during the course of the annual cycle, the summer hemisphere branch dominates. The annual cycle of the ITCZ over South America displays the least amount of symmetry with respect to north–south migration and ITCZ intensity. The surface underlying the ITCZ is largely responsible for this asymmetry as mentioned in the previous section. In this region, the phase of the ITCZ is locked to the annual cycle during its northward propagation, that is, when moving from south to north. However, after having reached the oceanic region north of South America, the convection diminishes slightly, and the cycle appears to lag slightly until the rainy season begins again over the Amazon

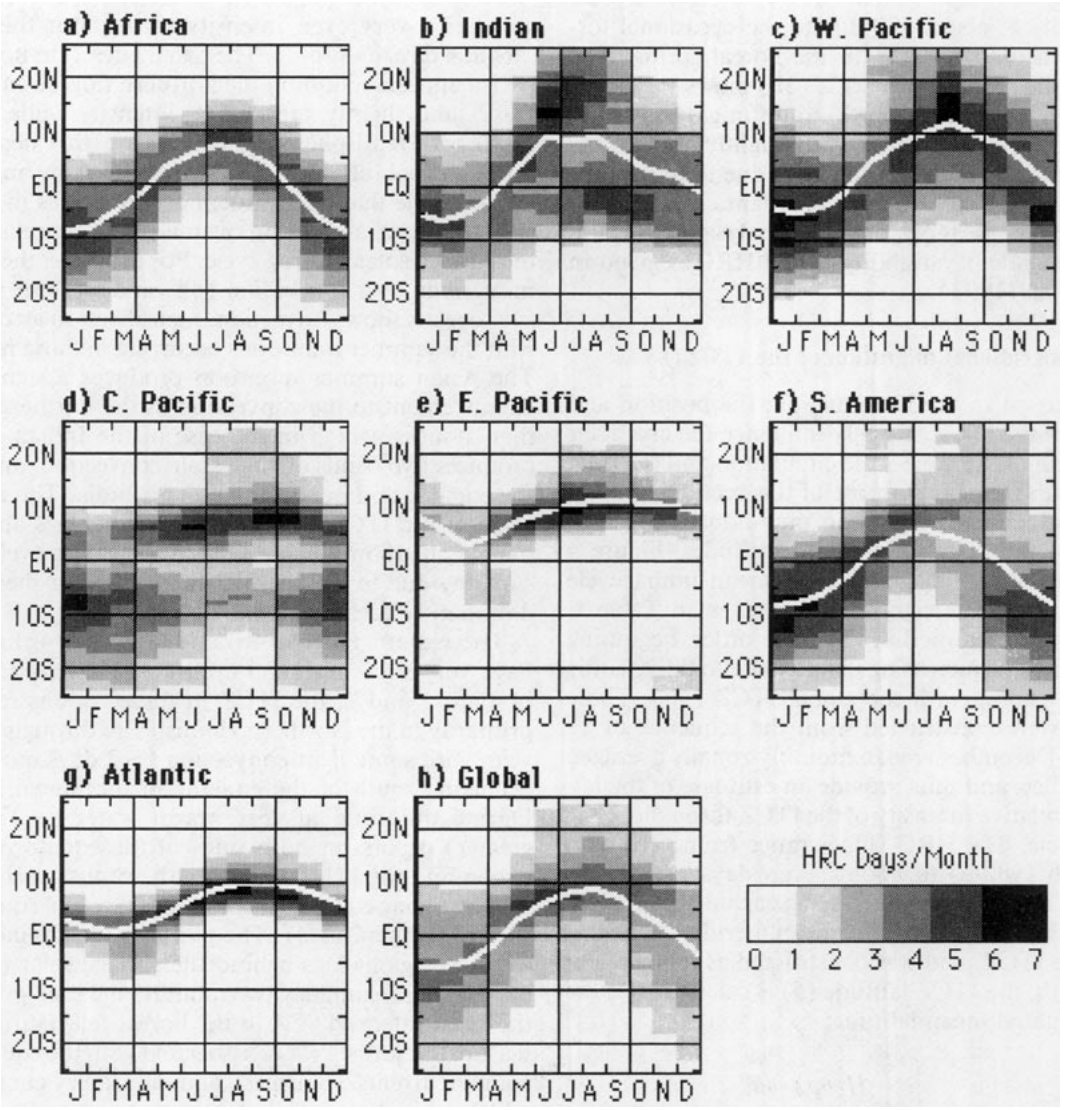

FIG. 4. Time–latitude diagrams of the annual cycle of ITCZ migration for the eight regions specified in Table 1. Annual cycles were computed from the 17 years of HRC data. White lines are quantitative estimates of the mean monthly ITCZ position (except central Pacific region); see text for computation.

Basin in November/December. For more in-depth analyses and discussion of the annual cycles in the Pacific and South American regions, the reader is referred to Horel (1982), Horel et al. (1989), and Mitchell and Wallace (1992).

The annual cycle of the global ITCZ has a modest resemblance to a sinusoidal pattern, with the intensity of the convection being strongest during the boreal summer and fall (5 days month^{-1}), and weakest during the equinoxes (3+ days month^{-1}). The nature of this off-equatorial enhancement reflects, in part, the fact that over much of the oceanic domain, equatorial upwelling introduces a region of relatively cool surface water along the equator. Thus, even though surface solar heating is strongest at the equator during the equinoxes, the relatively low SSTs at the equator (in a zonal-mean sense) combined with positive poleward SST gradients, do not support large-scale convection over the equator as readily as do the warm regions to the north and/or south. As mentioned earlier, further considerations regarding this feature of the ITCZ have been made by Charney (1971), Holton et al. (1971), Lindzen (1974), Lindzen and Hou (1988), Hess et al. (1993), and Waliser and Somerville (1993).

6. Anomalous fluctuations in ITCZ latitude and intensity

In this section, the analysis of the ITCZ migration patterns is extended to examine the anomalous fluctuations of ITCZ convection intensity and ITCZ latitude. Figure 5 contains time–latitude diagrams of HRC

anomalies about the annual cycles shown in Fig. 4, for the eight domains given in Table 1. The scale ranges from -3 days month^{-1} (white) to $+4$ days month^{-1} (black). Smoothing was applied to the diagrams in both the time and latitude dimensions using a three-month and three-degree box filter.

The time–latitude diagram of HRC anomalies for Africa (5a) suggests that most anomalies in convection tend to be associated with the strengthening or weakening of the ITCZ in its expected mean position (Fig. 4a), rather than anomalous convective events occurring away from the mean position. The strongest negative HRC anomalies occur in 1973, 1978, and 1981 while the strongest positive HRC anomalies occur in 1984 and 1987. The temporal extent of these strong anomalies is generally between 1 and 2 years. It should be noted that Gadgil et al. (1992) [cf. Chelliah and Arkin (1992)] have reported a systematic negative bias in the OLR dataset beginning in 1982 onward (their dataset extended to 1985) arising from changes in instruments, equatorial crossing times, etc. This bias may account for some of the positive HRC anomalies[2] occurring after 1982 since the HRC is constructed from both visible data, and the infrared data used to construct the OLR.

The anomalous HRC fields for the Indian and west Pacific regions (Figs. 5b and 5c) show long-term variability similar to that shown for Africa although it includes more variability at shorter time scales. Considerable variability at about one to three months was evident in the unsmoothed data (not shown). This shorter-term variability is largely attributable to the intraseasonal variability that has been found to prevail over the Indian and western Pacific oceans (e.g., Madden and Julian 1971; Lau and Chan 1988; Waliser et al. 1993). The Indian region (5b) shows significant anomalies north of 10°N that appear to be associated with the interannual variability in the strength and inland extent of the summer Asian monsoon. Somewhat similar behavior is noted for both the north and south summer monsoons of the western Pacific (i.e., southern Asia and northern Australia). In addition, the western Pacific shows strong negative equatorial anomalies in 1972 and 1982–83 associated with the particularly strong El Niño–Southern Oscillation (ENSO) events in those years (Rasmusson and Wallace 1983).

For the case of the central Pacific (5d), the anomalous HRC is dominated by negative and positive anomalies on or near the equator. The positive (negative) anomalies are associated with the warm (cold) phases of the ENSO cycle. For example, positive HRC anomalies are found on the equator in 1972, 1976–77, 1982–83, and 1987. The negative HRC anomalies are found in between these years, with the strongest occurring in 1972, 1973–75, 1981, and early 1984. In most cases, these negative anomalies coincide with episodes of strong equatorial upwelling in the central Pacific. The figure (5d) also shows considerable variability within the SPCZ between 10° and 25°S, which in most cases is out of phase with the anomalies near the equator.

The HRC anomaly field for the eastern Pacific (5e) shows a temporal pattern of interannual variability nearly identical to that of the equatorial central Pacific (5d). Again, this interannual signal is dominated by the climate anomalies associated with ENSO. This figure emphasizes the strength of the 1982–83 ENSO and the eastward extent of its influence. As shown in the figure, another aspect of interannual variability in this region is the strengthening or weakening of the "double" ITCZ in the boreal spring (see Fig. 4e).

The anomalies in convection for South America (5f) appear to be mostly in phase and of nearly the same magnitude as those of the other land case, Africa (5a). However, in contrast to the case of the ITCZ over Africa, the anomalies occur at latitudes other than the expected mean latitude of the ITCZ (4f). This is likely in part due to the larger irregularities in surface type and surface conditions over the South America region compared to Africa. The character of the HRC anomalies in the Atlantic (5g) is very similar to those of the eastern Pacific (5e); however, the anomalies are not in phase with those of the eastern Pacific, nor are they as strong. Further, there is more variability on and south of the equator in the Atlantic. Finally, the global ITCZ (5h) shows that anomalies for the globally averaged ITCZ generally fall between about ± 1 day month^{-1}, or about 25% of the annual cycle, and appear to have time scales of variability on the order of a few months to a few years. As mentioned earlier, the positive anomalies in convection occurring after 1982 may in part be due to the biases in the infrared satellite data reported by Gadgil et al. (1992) and Chelliah and Arkin (1992).

Figure 6 contains time series of ITCZ latitude anomalies. These time series represent the departures of the monthly ITCZ positions (calculation described in previous section) from the mean annual cycles shown in Fig. 4 (white lines). The time series shown were smoothed with a three-month box filter. As noted earlier, the computation does not apply to the double-banded structure of the central Pacific, and therefore a time series for this region is not included.

The time series for Africa (6a) shows maximum departures in the meridional position of the ITCZ of about 2°, with the largest excursions being northward anomalies. The time series exhibits significant variability at time scales of about 3–18 months (hereafter "high" frequency), in which most anomalies last about a season, and the different "events" are separated by anywhere between 6 and 18 months. There is also an

[2] In relation to deep convection anomalies, HRC and OLR anomalies have the opposite sign, with HRC having the same sign as deep convection.

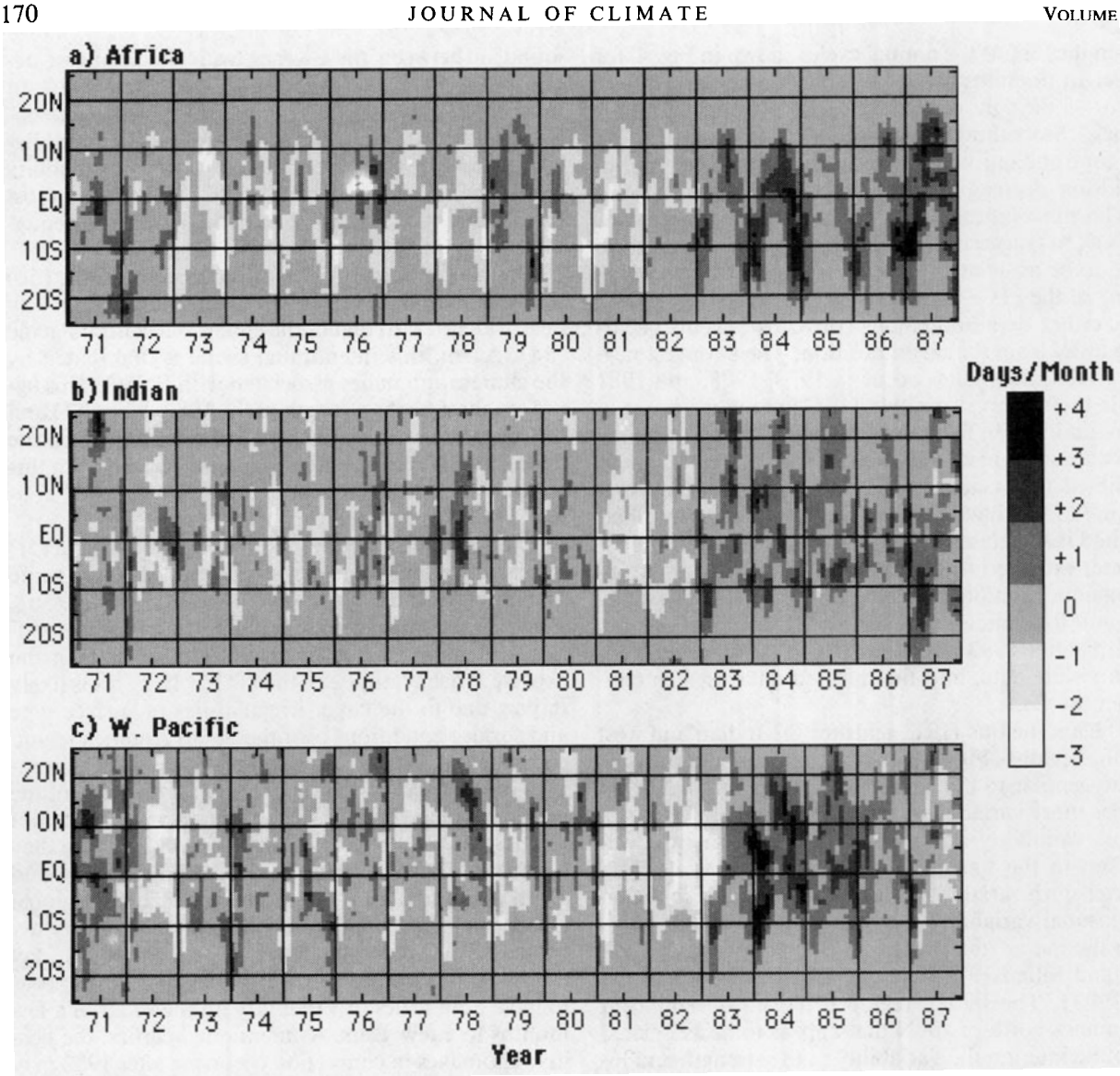

FIG. 5. Time–latitude diagrams of the monthly anomalies in convection (HRC) for the eight regions specified in Table 1, about the annual cycles shown in Fig. 4. Smoothing was applied to the data in both the time and latitude dimensions using a three-month and three-degree box filter.

indication of a "low-" frequency oscillation in which the ITCZ tended to be more northward in the middle part of the record, and more southward in the early seventies and middle eighties.

The time series for the Indian region (6b) is similar in character to the Africa region (6a) except 1) the largest anomalies are negative and occur during southward excursions, 2) there is slightly more "high-" frequency variability, and 3) there does not appear to be a "low-" frequency oscillation in the time series. The time series for the western Pacific region (6c) shows larger excursions (2°–4°) lasting for much longer periods (6–12 months). It is interesting to note that during the 1982–83 ENSO event, the western Pacific ITCZ made a strong transition from being anomalously north to anomalously south of its climatological position. By examining the mean annual cycle (Fig. 4c), it can be seen that most of this behavior is a reflection of the western Pacific ITCZ avoiding the equatorial region. This may be due to the large-scale, positive convective anomalies in the central Pacific region (Fig. 5d) causing a slight suppression of the convection in the western Pacific.

The time series of ITCZ latitude anomalies for the eastern Pacific region (6d) is dominated by the 1982–83 negative anomaly, which shows the ITCZ to be about 6° south of its climatological position for several months near the beginning of 1983. Further interesting behavior in this anomaly time series can be seen when compared to the western Pacific (6c). With the excep-

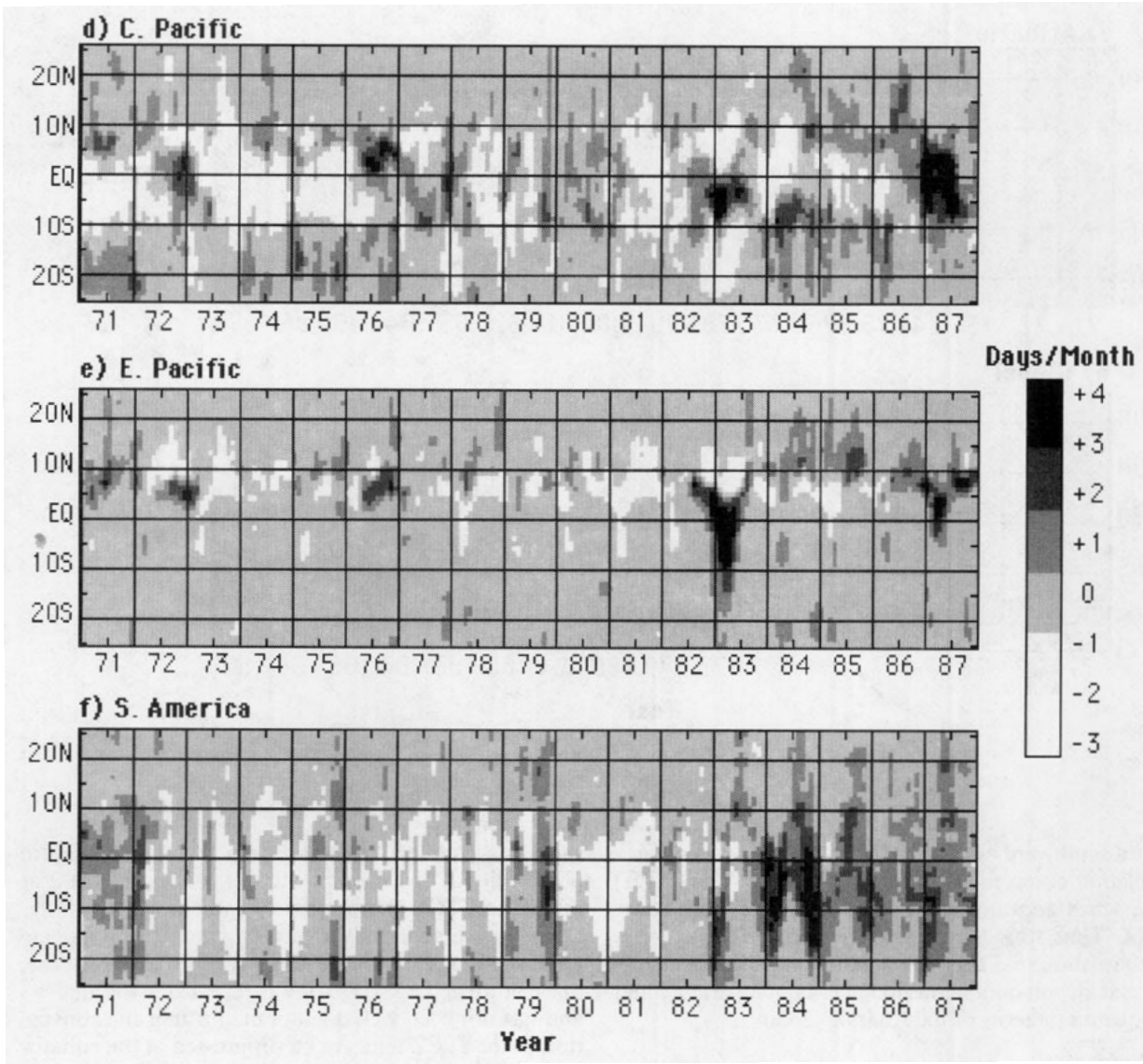

tion of the 1982–83 anomaly, many of the more modest anomalies within these two regions, which are on the order of 1°–2°, appear to be directly out of phase. This behavior is likely due to the coupling between these two regions via the east–west circulation of the Walker cell (e.g., Bjerknes 1969), whereby a positive convection anomaly in one region produces a negative convection anomaly in the other, which for these time series may show up as an anomalous latitude shift of the ITCZ.

The latitude anomalies for the South American region (6e) show anomalous excursions that are frequently on the order of 3° or more. There is significant variability on seasonal time scales that likely reflects the inhomogeneous surface boundary conditions and different climatological regimes in this region, conditions that make the "ITCZ" in this region less amenable to the procedures used to discern a "linear" ITCZ within the given longitude domain. However, the latitude anomalies for the Atlantic region (6f), which has a well-defined ITCZ, are modestly correlated with those of South America ($r = 0.41$; $N = 202$). Maximum anomalies in this region are about 2° at mostly seasonal time scales. As with Africa (6a), there appears to be a low-frequency oscillation in which the ITCZ is generally northward of its climatological position in the middle of the record presented and southward in the early seventies and middle eighties.

Finally, the time series of latitude anomalies of the global ITCZ (6g) shows very modest anomalies, mostly on the order of 1°, and two that are about 2°. The first of these was a positive anomaly in the middle of 1979 when the ITCZ was already near a northward extreme, the second was a negative anomaly when the ITCZ was

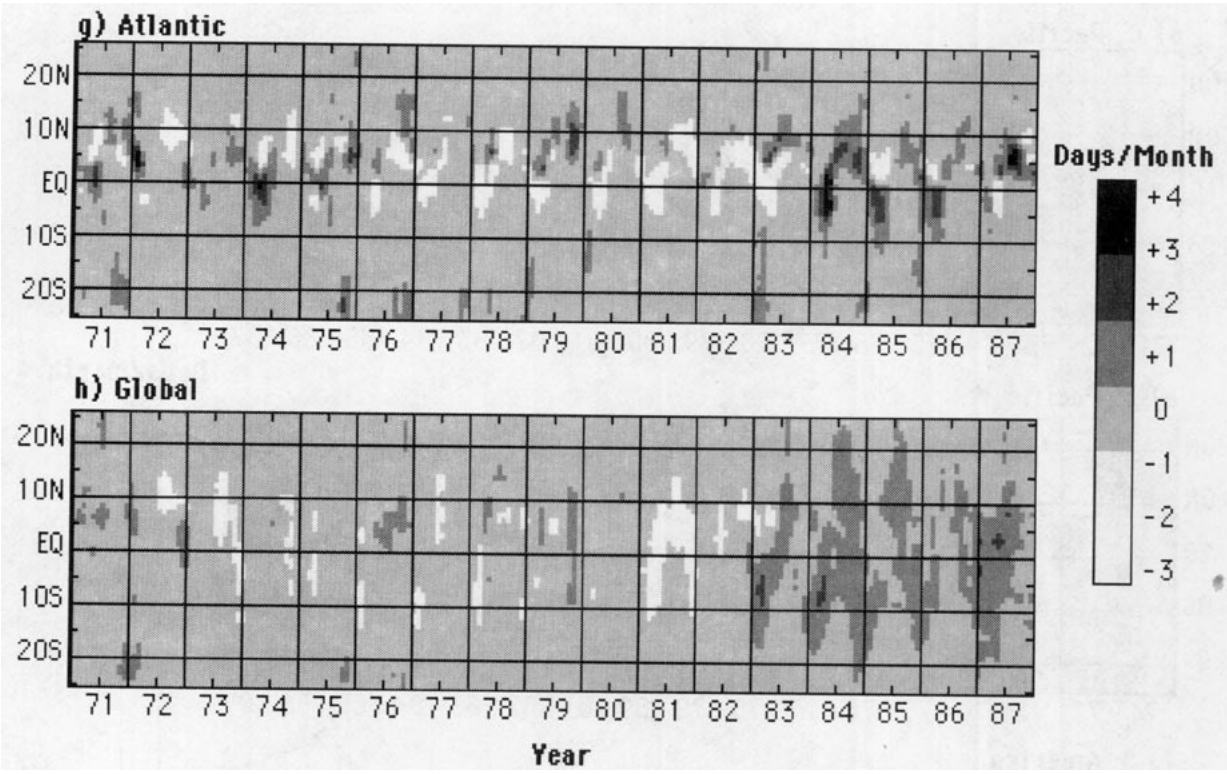

FIG. 5. (*Continued*)

near a southward extreme (Fig. 4h). The low-frequency oscillation observed in the Africa (6a) and Atlantic (6f) time series does not readily appear in the global time series. Thus, this long-period "oscillation" may be a manifestation of a regional climate fluctuation, possibly associated with anomalous long-period temperature and circulation patterns of the Atlantic Ocean.

7. Summary

The objective of this paper is to present fundamental characteristics of the global ITCZ in a simple and concise manner. The features provided by the HRC dataset afford an ideal opportunity to document essential ITCZ features such as the mean horizontal structure, the all-important meridional migration patterns, and the seasonal and interannual variability of the convection within, and latitude of, the ITCZ. This type of analysis, utilizing such a long-period (17 years) and well-suited dataset, has been rare. Many generalized cloud atlases and climatologies have been developed and analyzed but these types of analyses are usually deficient for those interested in singling out the characteristics and nuances of the ITCZ(s). We have tried to distill into this analysis the most basic characteristics of the ITCZ, and include some new material such as the long-record anomalous fluctuations in ITCZ convection and mean latitude. Within the context of a more comprehensive ITCZ study itself (Waliser 1992), it is hoped that this short presentation can serve as a resource to future observational or modeling studies concerned with, or related to, ITCZ characteristics and climatology.

While the analysis was not designed to investigate uncharted territory or resolve any particular issue(s), one feature of the ITCZ that was revealed in the analysis and has not been well documented is that the convection in the ITCZ tends to be suppressed at the equator over warm ocean regions of the tropics. This feature has been known to exist in regions such as the eastern Pacific and Atlantic where strong easterly trades force significant equatorial ocean upwelling. However, its existence in the warm-pool regions, that is, Indian and west Pacific oceans, has not been readily established, particularly on long time scales. The presence of an equatorial "dry zone" in regions where the SST tends to be maximum on the equator suggests that a dynamical mechanism originating in the atmosphere is acting to enhance convection away from the equator. This mechanism may be important in determining the overall latitude preference of the ITCZ (about 6°N; Fig. 2h) and thus the near-equatorial tropical wind field. The establishment and documentation of this feature is important in evaluating the theories put forward that attempt to explain the off-equatorial preference of the ITCZ as well as in assessing the performance of moist convection parameterizations in the near-equatorial regions.

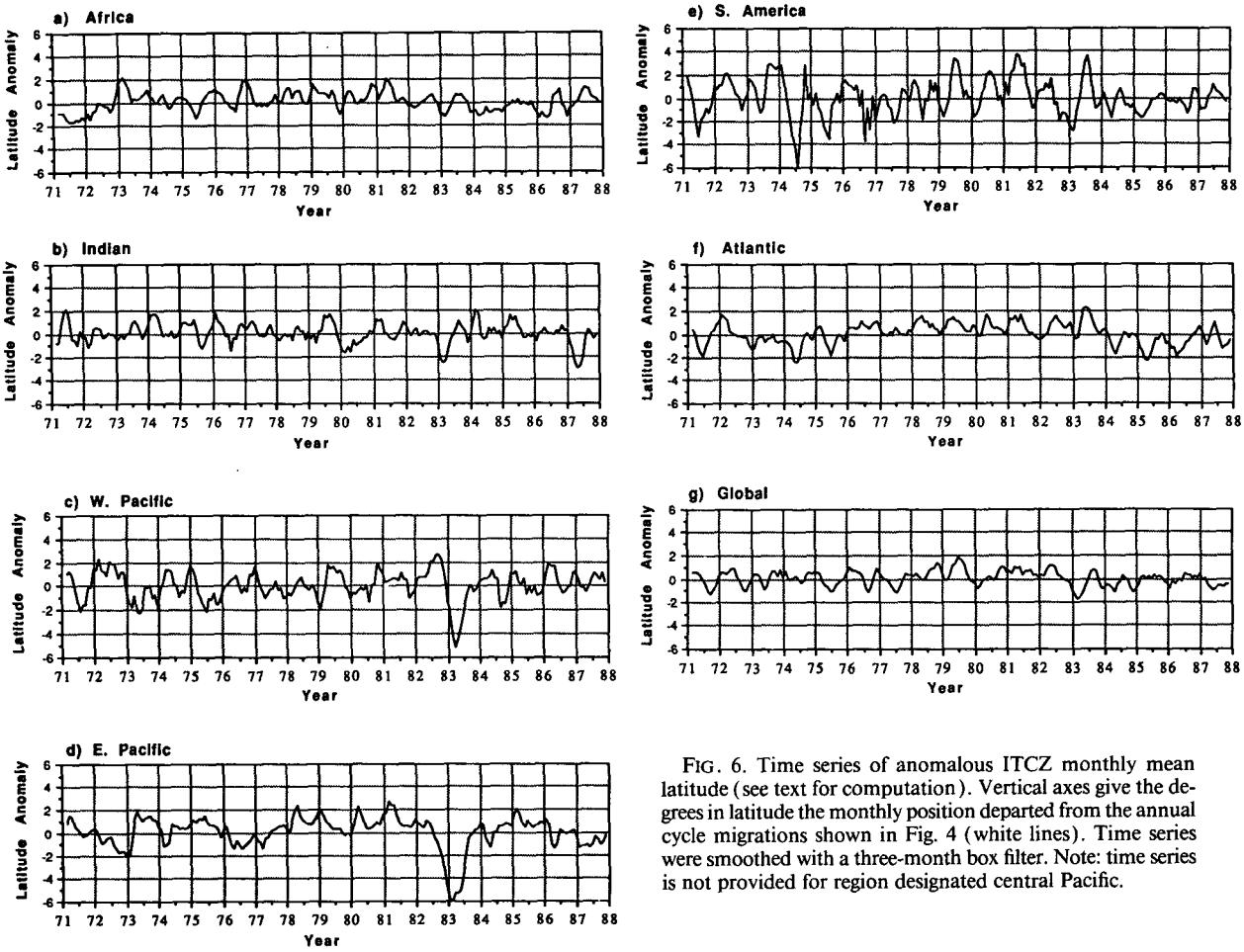

FIG. 6. Time series of anomalous ITCZ monthly mean latitude (see text for computation). Vertical axes give the degrees in latitude the monthly position departed from the annual cycle migrations shown in Fig. 4 (white lines). Time series were smoothed with a three-month box filter. Note: time series is not provided for region designated central Pacific.

This analysis of the long-record ITCZ latitude series provided estimates of the anomalous latitude excursions of the ITCZ on monthly to interannual time scales. Departures from mean annual migrations were found to be as great as 6° on a regional basis, and up to almost 2° for the globally averaged ITCZ. These anomalous excursions have typical time scales of 3–18 months for the monthly data (smoothed with a three-month box filter). Also evident from this analysis was a very long-period "oscillation" in the ITCZ latitude series for the Africa and Atlantic regions that suggests that the ITCZ was anomalously northward by about 0.5° during the late seventies and early eighties, and anomalously southward by about the same amount during the early 1970s and middle 1980s. This type of long-period "oscillation" may possibly be related to long-period variability associated with the temperature and circulation of the Atlantic Ocean. The understanding of the mechanisms behind these types of ITCZ latitude fluctuations and even an understanding of why the ITCZ in its "mean" state favors the Northern Hemisphere are still areas under investigation.

Acknowledgments. The authors would like to acknowledge the helpful comments and suggestions from two anonymous reviewers. This research was supported by the NASA Graduate Research Fellowship Program under Grant NGT-50304, the California Space Institute under Minigrants CS-88-89 and CS-45-90, and NOAA under Grant NA16RC0524-01.

REFERENCES

Asnani, G. C., 1968: The equatorial cell in the general circulation. *J. Atmos. Sci.*, **25**, 133–134.

Bates, J. R., 1970: Dynamics of disturbances on the Intertropical Convergence Zone. *Quart. J. Roy. Meteor. Soc.*, **96**, 677–701.

Bjerknes, J., L. J. Allison, E. R. Kreins, F. A. Godshall, and G. Warnecke, 1969: Satellite mapping of the Pacific tropical cloudiness. *Bull. Amer. Meteor. Soc.*, **50**, 313–322.

Bjerknes, J., 1969: Atmospheric teleconnections from the equatorial Pacific. *Mon. Wea. Rev.*, **97**, 163–172.

Charney, J. G., 1971: Tropical cyclogenesis and the formation of the Intertropical Convergence Zone. *Mathematical Problems of Geophysical Fluid Dynamics, Lectures in Applied Mathematics*, Vol. 13, W. H. Reid, Ed., Amer. Math. Soc., 355–368.

Chelliah, M., and P. Arkin, 1992: Large-scale interannual variability of monthly outgoing longwave radiation anomalies over the global oceans. *J. Climate*, **5**, 371–389.

Estoque, M. A., and M. Douglas, 1978: Structure of the intertropical convergence zone over the GATE area. *Tellus,* **30,** 55–61.

Fletcher, R. D., 1945: The general circulation of the tropical and equatorial atmosphere. *J. Meteor.,* **2,** 167–174.

Flohn, H., 1971: Tropical circulation patterns. *Bonner Meteor. Abhand.,* **15,** 55 pp.

Frank, W. M., 1983: The structure and energetics of the east Atlantic intertropical convergence zone. *J. Atmos. Sci.,* **40,** 1916–1929.

Gadgil, S., and A. Guruprasad, 1990: An objective method for identification of the intertropical convergence zone. *J. Climate,* **3,** 558–567.

——, A. Guruprasad, and J. Srinivasan, 1992: Systematic bias in the NOAA Outgoing Longwave Radiation Dataset. *J. Climate,* **5,** 867–875.

Garcia, O., 1985: Atlas of highly reflective clouds for the global tropics: 1971–1983. *U.S. Dept. of Commerce, NOAA,* Environmental Research Lab., Boulder, Co, 365 pp. [NTIS PB-87129169.]

Goswami, B. N., J. Shukla, E. K. Schneider, and Y. C. Sud, 1983: Study of the dynamics of the intertropical convergence zone with a symmetric version of the GLAS climate model. *J. Atmos. Sci.,* **41,** 5–19.

Graham, N. E., and T. P. Barnett, 1987: Sea surface temperature, surface wind divergence, and convection over tropical oceans. *Science,* **238,** 657–659.

Gruber, A., 1972: Fluctuations in the position of the ITCZ in the Atlantic and Pacific oceans. *J. Atmos. Sci.,* **29,** 193–197.

——, and A. F. Krueger, 1984: The status of the NOAA Outgoing Longwave Radiation Data Set. *Bull. Amer. Meteor. Soc.,* **65,** 958–962.

Hack, J. J., W. H. Shubert, D. E. Stevens, and H. C. Kuo, 1989: Response of the Hadley Circulation to convective forcing in the ITCZ. *J. Atmos. Sci.,* **46,** 2957–2973.

Hastenrath, S. L., 1968: On mean meridional circulations in the tropics. *J. Atmos. Sci.,* **25,** 979–983.

Hess, P. G., D. S. Batissti, and P. J. Rasch, 1993: Maintenance of the intertropical convergence zones and the large-scale circulation on a water-covered earth. *J. Atmos. Sci.,* **50,** 691–713.

Holton, J. R., J. M. Wallace, and J. A. Young, 1971: On boundary layer dynamics and the ITCZ. *J. Atmos. Sci.,* **28,** 275–180.

Horel, J., 1982: On the annual cycle of the tropical Pacific atmosphere and ocean. *Mon. Wea. Rev.,* **110,** 1863–1877.

——, A. N. Hahmann, and J. E. Geisler, 1989: An investigation of the annual cycle of convective activity over the tropical Americas. *J. Climate,* **2,** 1388–1403.

Hubert, L. F., A. F. Krueger, and J. S. Winston, 1969: The double intertropical convergence zone—Fact or fiction? *J. Atmos. Sci.,* **26,** 771–773.

Kilonsky, B. J., and C. S. Ramage, 1976: A technique for estimating tropical open-ocean rainfall from satellite observations. *J. Appl. Meteor.,* **15,** 972–976.

Kornfield, J., A. F. Halser, K. J. Hanson, and V. E. Suomi, 1967: Photographic cloud climatology from ESSA III and V computer produced mosaics. *Bull. Amer. Meteor. Soc.,* **48,** 878–883.

Kraus, E. B., 1977: The seasonal excursions of the intertropical convergence zone. *Mon. Wea. Rev.,* **105,** 1009–1018.

Lau, K. M., and P. H. Chan, 1988: Intraseasonal and interannual variations of tropical convection: A possible link between the 40–50-day oscillation and ENSO? *J. Atmos. Sci.,* **45,** 506–521.

Legler, D. M., and J. J. O'Brien, 1984: *Atlas of tropical pacific wind stress climatology 1971–1980.* Dept. of Meteor, Florida State Univ., 82 pp.

Levitus, S., 1982: *Climatological Atlas of the World Ocean.* NOAA Prof. No. Paper 13. U.S. Govt. Printing Office, Washington, D.C., 173 pp. [Available from U.S. Department of Commerce, NOAA, Rockville, MD.]

Liebmann, B., and H. H. Hendon, 1990: Synoptic-scale disturbances near the equator. *J. Atmos. Sci.,* **47,** 1463–1479.

Lindzen, R. S., 1974: Wave-CISK in the Tropics. *J. Atmos. Sci.,* **31,** 156–179.

——, and A. Y. Hou, 1988: Hadley circulation for zonally averaged heating centered off the equator. *J. Atmos. Sci.,* **45,** 2416–2427.

Madden, R., and P. R. Julian, 1971: Detection of a 40–50-day oscillation in the zonal wind in the tropical Pacific. *J. Atmos. Sci.,* **28,** 702–708.

Mitchell, T. P., and J. M. Wallace, 1992: On the annual cycle in equatorial convection and sea surface temperature. *J. Climate,* **5,** 1140–1156.

Oort, H., 1983: Global atmospheric circulation statistics, 1958–1973. NOAA Professional Paper 14. U.S. Govt. Printing Office, Washington, D.C.

Pike, A. C., 1972: The inter-tropical convergence zone studied with an interacting atmosphere and ocean model. *Mon. Wea. Rev.,* **99,** 469–477.

Ramage, C. S., 1981: The central Pacific near-equatorial convergence zone. *J. Geophys. Res.,* **86,** No. C7, 6580–6598.

Rasmusson, E. M., and J. M. Wallace, 1983: Meteorological aspects of the El Niño/Southern Oscillation. *Science,* **222,** 1195–1202.

Reed, R. J., and E. E. Recker, 1971: Structure and properties of synoptic-scale wave disturbances in the equatorial western Pacific. *J. Atmos. Sci.,* **28,** 1117–1133.

Reynolds, R. W., 1988: A real-time global sea surface temperature analysis. *J. Climate,* **1,** 75–86.

Rossow, W. B., and R. A. Schiffer, 1991: ISCCP cloud data products. *Bull. Amer. Meteor. Soc.,* **72,** 2–20.

Schneider, E. K., and R. S. Lindzen, 1977: Axially symmetric steady-state for instability and climate studies. Part I. Linearized calculations. *J. Atmos. Sci.,* **34,** 263–279.

Simpson, R. H., 1947: Synoptic aspects of the intertropical convergence near Central and South America. *Bull. Amer. Meteor. Soc.,* **24,** 335–346.

Waliser, D. E., 1992: The preferred latitudes of the intertropical convergence zone: Observations and theory. Ph.D. dissertation, Scripps Institution of Oceanography, University of California, San Diego, 170 pp. [Available from UCSD, La Jolla, CA 92093.]

——, and R. C. J. Somerville, 1993: The preferred latitudes of the intertropical convergence zone. *J. Atmos. Sci.,* submitted.

——, N. E. Graham, and C. Gautier, 1993: Comparison of the highly reflective cloud and outgoing longwave radiation datasets for use in estimating tropical deep convection. *J. Climate,* **6,** 331–353.

Wallace, J. M., 1971: Spectral studies of tropospheric wave disturbances in the tropical western Pacific. *Rev. Geophys. Space Phys.,* **9,** 557–611.

Webster, P. J., 1987: The Interactive Monsoon. *Monsoons,* J. S. Fein and P. L. Stephens, Eds. Wiley-Interscience, 269–330.

Winston, J. S., 1971: The annual course of zonal mean albedo as derived from ESSA 3 and 5 digitized picture data. *Mon. Wea. Rev.,* **99,** 818–827.

Yanai, M., T. Maruyama, T. Nitta, and Y. Hayashi, 1968: Power spectra of large scale disturbances of the tropical Pacific. *J. Meteor. Soc. Japan,* **46,** 308–323.